Mass spectrometry-based discovery of circadian peptides

Nathan G. Hatcher*†, Norman Atkins, Jr.‡, Suresh P. Annangudi*†, Andrew J. Forbes*, Neil L. Kelleher*§, Martha U. Gillette‡§¶, and Jonathan V. Sweedler*†‡§ ‖

*Department of Chemistry; †Beckman Institute; ‡Neuroscience Program; ¶Department of Cell and Developmental Biology; and §Institute for Genomic Biology, University of Illinois, Urbana, IL 61801

Communicated by William T. Greenough, University of Illinois at Urbana–Champaign, Urbana, IL, May 20, 2008 (received for review January 18, 2008)

A significant challenge to understanding dynamic and heterogeneous brain systems lies in the chemical complexity of secreted intercellular messengers that change rapidly with space and time. Two solid-phase extraction collection strategies are presented that relate time and location of peptide release with mass spectrometric characterization. Here, complex suites of peptide-based cell-to-cell signaling molecules are characterized from the mammalian suprachiasmatic nucleus (SCN), site of the master circadian clock. Observed SCN releasates are peptide rich and demonstrate the corelease of established circadian neuropeptides and peptides with unknown roles in circadian rhythms. Additionally, the content of SCN releasate is stimulation specific. Stimulation paradigms reported to alter clock timing, including electrical stimulation of the retinohypothalamic tract, produce releasate mass spectra that are notably different from the spectra of compounds secreted endogenously over the course of the 24-h cycle. In addition to established SCN peptides, we report the presence of proSAAS peptides in releasates. One of these peptides, little SAAS, exhibits robust retinohypothalamic tract–stimulated release from the SCN, and exogenous application of little SAAS induces a phase delay consistent with light-mediated cues regulating circadian timing. These mass spectrometry-based analyses provide a new perspective on peptidergic signaling within the SCN and demonstrate that the integration of secreted compounds with information relating time and location of release generates new insights into intercellular signaling in the brain.

little SAAS | neuropeptides | solid-phase extraction | peptidomics | suprachiasmatic nucleus

A fundamental component of cell-to-cell signaling in the brain is the release of endogenously derived neuropeptide-based transmitters and modulators within dynamic neural networks. Neuropeptides include a broad set of structurally diverse molecules that are physiologically active at low concentrations and localize across heterogeneous brain regions, particularly throughout neuroendocrine systems. These properties contribute marked chemical complexity to neurotransmission within heterogeneous and dynamic brain systems. Directly acquiring releasate information about chemical content, release site distribution, and stimulation dependence is a significant challenge to the study of neuronal networks incorporating neuropeptide intercellular signaling.

This article describes the use of several unique peptide sampling approaches to characterize chemically complex releasates from the rat suprachiasmatic nucleus (SCN), the site of the master circadian clock (1, 2). The SCN is highly innervated with peptidergic efferents, afferents, and interneurons (3). Moreover, SCN humoral signals are critical elements for the coordination of biological rhythms because SCN transplants can restore aspects of circadian rhythms in SCN-ablated animals (4). In the present work, SCN releasates were collected and concentrated directly from brain slices using either solid-phase extraction (SPE) material embedded within pipettes or micrometer-sized SPE beads that function as region-specific sampling probes (5–8). Captured releasates then were characterized offline with MALDI TOF MS. Following this strategy, releasates could be screened for multiple compounds that include known, unexpected, or even unknown compounds.

We characterized peptides endogenously secreted from the site of the SCN over the course of 24 h as well as peptides released specifically following electrophysiological stimulation of the retinohypothalamic (RHT) tract, the afferent pathway mediating SCN phase-setting light cues (9, 10). Surprisingly complex SCN neuropeptide release spectra were observed with the use of a combination of neurophysiology and selective sampling. In addition to established SCN peptides, we detected RHT-dependent secretion of proSAAS-derived peptides, namely PEN, big LEN, and little SAAS. Following this finding, we demonstrate that exogenous application of little SAAS induces a marked phase delay in SCN circadian rhythms.

NEUROSCIENCE

Results

To assess the peptide complement released in response to electrical stimulation of the RHT tract, brain slices containing the SCN and attached optic nerves were prepared for electrical stimulation. Extracellular samples of the SCN region were collected using an "on-tissue" collection strategy, illustrated in Fig. 1*A*. Briefly, C_{18}-containing Zip Tip (Millipore) pipette tips were positioned directly over the SCN region. Extracellular media were drawn through the embedded C_{18} material, allowing adsorption of extracellular compounds that subsequently were eluted for offline mass spectrometric analyses. Fig. 1*B* compares mass spectra of SCN releasates before and during electrophysiological stimulation of the RHT tract ($n = 8$). Multiple compounds were present only in the stimulation mass spectrum; the prestimulation mass spectra exhibited only a few analytes (e.g., thymosin β-4).

In contrast to the relatively few analytes observed in the prestimulation samples, collections obtained during and after stimulation yielded an abundance of peptides (Fig. 1*B*, *bottom spectrum*). Peaks were identified initially by matching the observed mass of the intact ion with the predicted masses of known peptides. These releasate peak assignments were within 50 ppm of the predicted mass. The first peak, at 1084.46 m/z, matched the predicted mass for arginine vasopressin (AVP), an established SCN neuropeptide (11, 12). Other known or suggested SCN-related neuropeptides were observed also (3, 10, 13–17). Notably, three proSAAS-derived peptides (18), little SAAS, big LEN,

Author contributions: N.G.H., A.J.F., N.L.K., M.U.G., and J.V.S. designed research; N.G.H., N.A., and S.P.A. performed research; N.G.H., N.A., S.P.A., A.J.F., M.U.G., and J.V.S. analyzed data; and N.G.H. and J.V.S. wrote the paper.

Conflict of interest statement: Dr. Greenough is a research collaborator with Dr. Sweedler on other, unrelated work. Also, Dr. Gillette was formerly the head of the Department of Cell and Developmental Biology, of which Dr. Greenough is a faculty member.

Freely available online through the PNAS open access option.

‖To whom correspondence should be addressed at: Department of Chemistry, University of Illinois, 71 Roger Adams Lab, 600 S. Mathews Avenue, Urbana, IL 61801. E-mail: jsweedle@uiuc.edu.

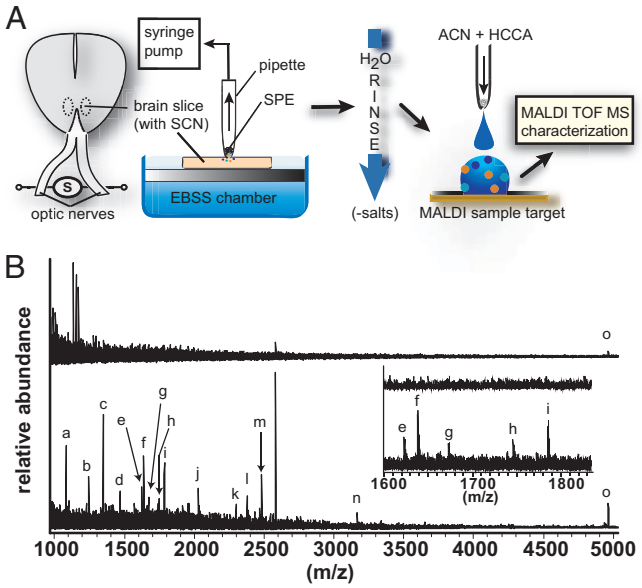

Fig. 1. Characterization of RHT-stimulated SCN releasates. (*A*) Sample collection and preparation. (*B*) MS characterization of SCN releasates. Inset shows a zoomed mass range highlighting compounds not clearly observable in the expanded spectrum. Labeled analytes are as follows: (a) AVP, (b) proSomatostatin 89–100, (c) substance P, (d) PENK 219–229, (e) melanotropin α, (f) somatostatin 14, (g) pyro-glu neurotensin, (h) big LEN, (i) little SAAS, (j) unknown 2028.02 *m/z*, (k) PEN, (l) unknown 2380.10 *m/z*, (m) unknowns 2481.26/2481.77 *m/z*, (n) galanin, and (o) thymosin β-4.

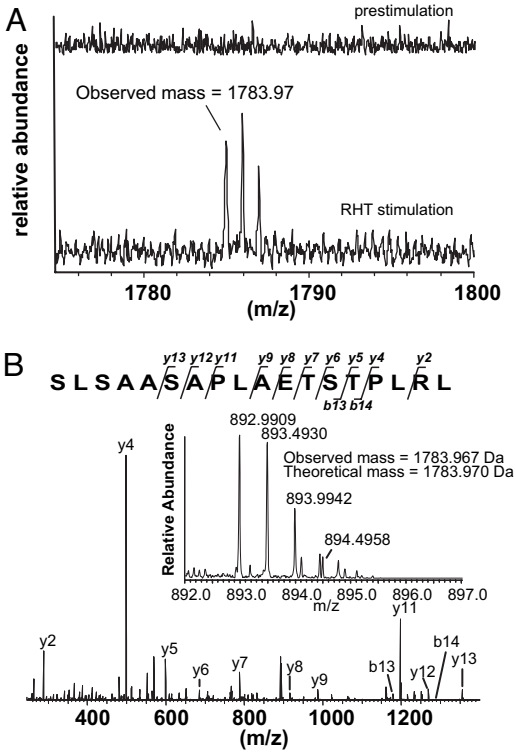

Fig. 2. MS/MS verification of releasate identities: little SAAS. (*A*) Comparison of prestimulation and RHT-stimulated releasates clearly shows the monoisotopically distributed peak matching the mass of little SAAS. Samples were collected with SPE pipettes as in Fig. 1. (*B*) Fourier transform MS of the same analyte obtained from extracts of isolated SCN explants shows almost the complete y ion series predicted by the sequence of little SAAS (*illustrated at the top*). Additional support for little SAAS identification follows from the intact ion spectrum (*inset*), which closely matches the predicted mass for little SAAS.

and PEN, with no known role in circadian rhythms, were clearly present in these RHT-stimulated releasates.

To verify the identity of putative mass matches in releasate samples, sequence information was acquired using tandem mass spectrometry (MS/MS) approaches. For most secreted analytes, the amounts of analyte collected from releasates were insufficient for MS/MS. To obtain sufficient amounts of these compounds, SCN tissue punches were subjected to peptide extraction protocols commonly used for MS-based peptidomic studies (19–21). Following separation of these extracts by liquid chromatography, analytes from the tissue-extracted samples were matched by mass to corresponding releasate analytes for MS/MS by MALDI TOF MS/MS and, in some instances, were matched separately by linear ion trap quadrupole Fourier transform mass spectrometry for sequence confirmation. Precursor and fragment ion masses were compared statistically against an in-house database of predicted masses and fragmentation patterns of rat neuropeptides.

Fig. 2 depicts this process for the peptide little SAAS. Releasate data obtained with pipette collections clearly delineated a stimulation-dependent analyte with an observed monoisotopic mass matching little SAAS. Fig. 2*B* shows the spectrum generated by Fourier transform mass spectrometry from the analyte extracted from the SCN that matched the little SAAS releasate; this value represented an accurate match to within 0.5 ppm. The product ion spectrum generated from additional MS/MS sequencing matched nearly all y-ions, confirming its identity. Following this strategy, we verified the identities of most peptides observed in releasate samples (Table 1).

We used micrometer-sized SPE beads as spatially selective collection probes (5) to test whether the releasates observed in Figs. 1 and 2 originated from the SCN. The SPE beads were composed of polymer resin (Millipore resin "D"), which binds peptides and proteins nonselectively through hydrophobic interactions. We tested the capability of single-bead collection to resolve release between established AVP-positive and AVP-negative regions of the preparation of the coronal-slice rat brain. AVP-expressing neurons and processes were found within the SCN and in the nearby supraoptic nucleus (SON) (22, 23). Beads were positioned on these regions and on the AVP-negative anterior hypothalamic (AHP) nucleus and optic tract (OT) region (Fig. 3). Beads were exposed to the slice surface for 20-min intervals before and during stimulation at circadian time (CT) 6 with elevated K^+ (55 mM KCl) in Earle's Essential Balanced Salt Solution (EBSS); tissues were stimulated for 5 min before washing with EBSS.

Mass spectra obtained from the stimulation releasate profiles had distinct differences in the SON, SCN, AHP, and OT regions, reflecting the distribution of AVP expression across the coronal slice (Fig. 3*A*, $n = 4$). AVP was observed only after stimulation and only from AVP-expressing SCN and SON regions; AVP was not detected in releasates from either the adjacent OT region or the more distant AHP region. Expanding the mass range (Fig. 3*B*) revealed SCN peptide profiles similar to those observed from the pipette-collected samples. These releasates included AVP, neurotensin, galanin, and notably, little SAAS; however, these releasate peaks were not as intense as those observed with the pipette approach. Although the SCN shell and core exhibit differences in peptidergic innervation, the mass spectra of bead-obtained releasates were nearly identical (data not shown), suggesting that this approach could not distinguish potential differences in peptide releasates from these closely positioned areas.

The SCN secretes many neuropeptides that follow distinct patterns of circadian release. The release spectrum of a 24-h collection from an unstimulated coronal SCN slice preparation

Table 1. Peptides detected in SCN releasate mass spectra

Peptide[a]	*m/z* (MH+) Observed	*m/z* (MH+) Theoretical	Sequence	MS/MS
Angiotensin I	1296.70	1296.69	DRVYIHPFHL	√
Arginine vasopressin[b]	1084.46	1084.46	C*YFQNC*PRG-NH_2	√
proEnkephalin 219–229	1466.63	1466.65	VGRPEWWMDYQ	—
Galanin	3163.60	3163.58	GWTLNSAGYLLGPHAIDNHRSFSDKHGLT-NH_2	—
Neurokinin-B	1210.63	1210.54	DMHDFFVGLM-NH_2	√
Neurotensin	1672.92	1672.92	pQLYENKPRRPYIL	√
POMC, melanotropin α	1622.77	1622.79	SYSMEHFRWGKPV-NH_2	—
PEN	2301.25	2301.24	AVDQDLGPEVPPENVLGALLRV	√
Big LEN	1745.96	1745.97	LENSSPQAPARRLLPP	√
Little SAAS	1784.97	1784.97	SLSAASAPLAETSTPLRL	√
Somatostatin-14[b]	1637.72	1637.71	AGC*KNFFWKTFTSC*	—
proSomatostatin 89–100	1244.57	1244.57	SANSNPAMAPRE	√
Substance P	1347.74	1347.74	RPKPQQFFGLM-NH_2	√
Thymosin β-4	4961.73	4961.49	AcSDKPDMAEIEKFDKSKLKKTETQEKNPLPSKETIEQ-EKQAGES	√

[a]Unknowns (*m/z*): 1481.73, 1495.75, 2028.02, 2380.00, 2481.26
[b]Asterisk denotes disulfide bond.

is shown in Fig. 4*A*. Stimulation-independent compounds observed from the previous experiments are not labeled because these compounds may not represent secreted peptides. Releasates were obtained from coronal SCN preparations at 4-h sampling durations beginning and ending at CT 0–4, 4–8, 8–12, 12–16, 16–20, and 20–24 ($n = 2$ preparations for each CT interval). AVP secretion over time was found to exhibit a circadian rhythm, with the largest mass peaks observed in samples obtained during subjective day (CT 0–12, Fig. 4*B*). These data replicate reports monitoring AVP secretion from rat SCN (11, 12). We observed the release patterns of multiple secreted peptides in the same experiment: AVP, angiotensin I, substance P, little SAAS, and an unknown secreted compound with 1492.75 *m/z*. AVP and the unknown 1492.75 *m/z* exhibited robust circadian release that followed opposite phase patterns. Substance P and little SAAS showed endogenous secretion levels that varied but were difficult to resolve because they were near the detection limits. Angiotensin I secretion appeared not to cycle.

Our analysis revealed robust release of little SAAS following RHT stimulation at CT 14 compared with its modest endogenous release rate described earlier. The RHT transmits light-mediated cues critical to synchronizing circadian timing with environmental light/day cycles. We were interested in evaluating whether little SAAS can induce phase-setting effects. We assayed the effect of an exogenous application of synthetic little SAAS on the rhythm of neural activity in the SCN by using extracellular recordings from the coronal SCN brain slice over an 18-h period. Firing rates of SCN pacemaker cells peak near midday (around CT 7, as shown in Fig. 5*A*, *top*), and this peak is a reliable measure of phase (24). Drop-wise application of a negative control, 1 nM AVP in EBSS to the SCN surface for 5-min exposures at CT 14, had no effect on the peak activity phase over the course of the following 24-h cycle (Fig. 5*A*, *middle*). Similar application of 1 nM of little SAAS at CT 14 delayed peak electrical activity by an average of 1.5 h in recordings (Fig. 5*A*, *bottom*). Applications of little SAAS concentrations as high as 100 μM also delayed phase (data not shown) but did not extend this delay beyond shifts observed with 1-nM stimulations. Phase-shift comparisons are summarized in Fig. 5*B*.

Discussion

In an effort to address the general problem of measuring spatial and temporal dynamics of chemically complex peptide signals in discrete brain regions, we developed methods that enable characterization of neuropeptide signaling, demonstrated with *ex vivo* assays of the SCN circadian clock as a model system. We used two sample-collection strategies coupled to offline mass spectrometry. In addition to using SPE beads as region-specific sampling probes as described previously (5–8), we developed a second sampling approach in which we used SPE pipettes as "on tissue" analyte traps to collect and concentrate extracellular compounds more effectively. This increased rate of analyte recovery results in improved detection limits for releasates and, by increasing sample amounts, improves the mass accuracies of detected compounds relative to the bead probes. As compared with the single bead approach, however, the pipette method results in a loss of spatial information necessary to determine the peptide release site. By using both approaches in hypothalamic brain slices, we identified multiple simultaneously secreted neuropeptides specifically from the SCN. Taken together, these MS-based releasate assays reveal the complexity of intercellular peptide signaling within the SCN and, more notably, provide a rapid screen for unexpected neuropeptides that will be characterized functionally by directed bioassays.

Many neuropeptides co-released following RHT stimulation in these experiments have reported roles consistent with regulation of SCN phase (10, 13–16, 25). Because SCN phase-setting responses to photic cues are clearly time dependent (26), the specific peptide content of RHT-stimulated releasates may represent the activation of multiple peptidergic systems specific to the time of stimulation. Thus, the releasates observed here after RHT stimulation at CT 14 probably will differ from those obtained after stimulation early in the day or late at night.

These releasate profiles may not be complete, because neuropeptides mediating photic input or intra-SCN synchronization, such as pituitary adenylate cyclase-activating peptide (27, 28), vasoactive intestinal polypeptide (29, 30), and gastrin-releasing peptide (31, 32), are not observed or, in the case of gastrin-releasing peptide, are not present in amounts sufficient to produce peak intensities that exceed our significance criterion. Release of these peptides may be dependent on specific stimulation parameters such as frequency, intensity, or time of day. Alternatively, some releasates may be present in amounts below our current limits of detection.

Perhaps the most striking finding in this study is the presence of unknown compounds, with masses not matching known peptides, in SCN releasates. These secreted compounds may be undocumented forms derived from known SCN peptides (i.e.,

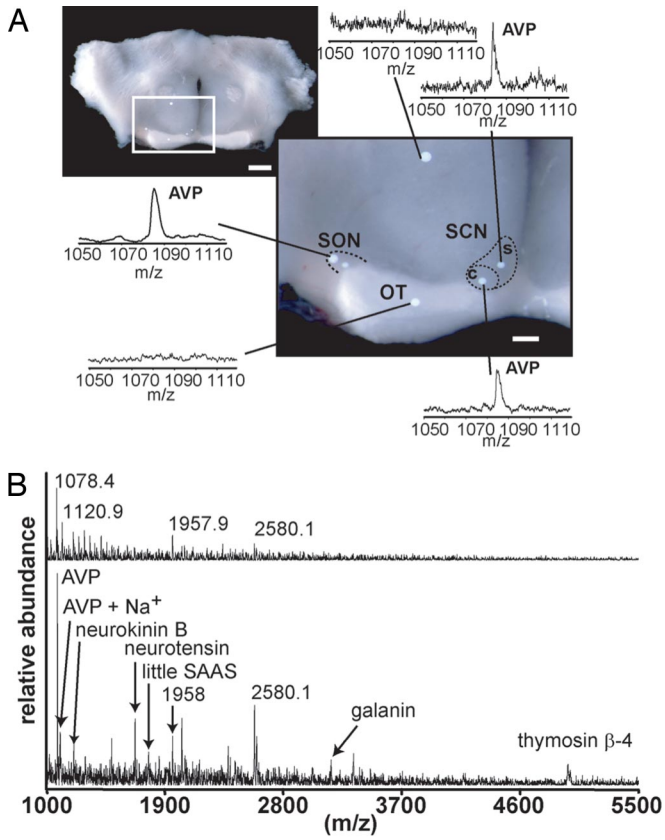

Fig. 3. Determining release from the SCN region with spatially resolved bead probes. (*A*) Beads are positioned at discrete locations on the coronal brain slice (scale bar, 1.0 mm). Discrete hypothalamic regions are outlined in this magnified image (scale bar, 0.2 mm) depicting beads on SCN, SON, AHP, and OT regions. Tissue is stimulated by spot application of elevated (55 mM) KCl-containing EBSS. AVP is present in the releasate mass spectra obtained from AVP-expressing SCN shell and core subregions and from SON but not from an adjacent AVP-negative OT region or a distant AHP area. (*B*) Comparisons of mass spectra obtained from prestimulation (*top*) and stimulation (*bottom*) bead collections over 20-min intervals from the SCN-positioned beads. Many stimulation-dependent compounds are clearly distinguishable from abundant analytes present in the prestimulation mass spectra and include many releasates similar to those observed with pipette collections, as in Fig. 1.

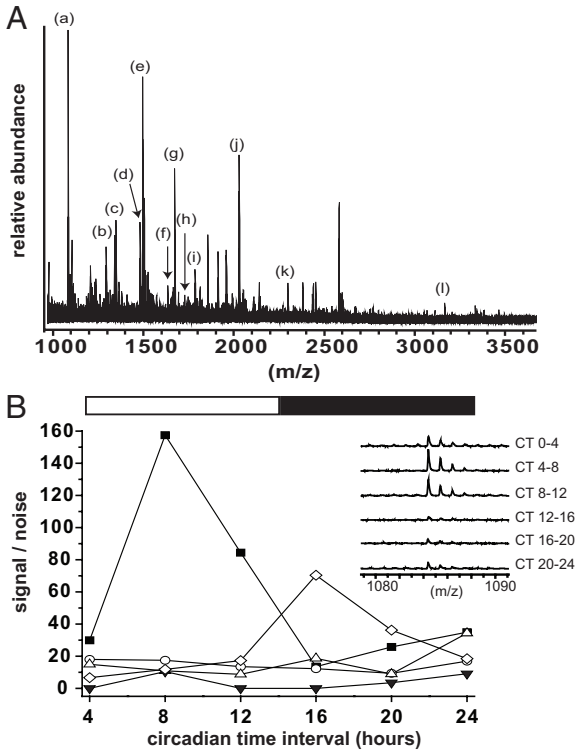

Fig. 4. Assays of endogenous circadian releasates. (*A*) Representative mass spectrum obtained over a 24-h collection period from an SCN brain slice. Analytes include (a) AVP, (b) angiotensin 1, (c) substance P, (d) unknown 1481.73 *m/z*, (e) unknown 1495.75 *m/z*, (f) somatostatin-14, (g) pyro-glu neurotensin, (h) big LEN, (i) little SAAS, (j) unknown 2028.02 *m/z*, (k) PEN, and (l) galanin. (*B*) Summary graph of the endogenous release of multiple analytes observed within the same 4-h collection mass spectra. Transparent and solid bars indicate subjective day and night, respectively (■ AVP, ○ angiotensin I, △ substance P, ▼ little SAAS, ◇ unknown at 1495.75 *m/z*). Inset: Endogenous release of AVP obtained over 4-h collection intervals. CT, circadian time.

proteolytic fragments of high-mass SCN peptides such as prokineticin 2 or unreported posttranslational modifications) or may, in fact, be secreted compounds that have not yet been identified. Once sequenced, these compounds can be assayed for physiological functions associated with circadian rhythms, as demonstrated here with the peptide little SAAS.

Discovery of the RHT-dependent secretion of little SAAS, big LEN, and PEN has far-reaching implications, because these peptides have not been examined in the context of circadian biology. We observed the activity-dependent co-release of proSAAS peptides from the brain slice and demonstrated a role for little SAAS in the regulation of circadian phase. Peptides derived from the C-terminal of proSAAS have been reported to regulate peptide processing within neuroendocrine cells (18, 33). However, findings from proSAAS-transfected AtT-20 cells suggest that proSAAS peptides are released and may function as neurohormones or possibly even as neurotransmitters (34). In rat, immunoreactivity of the proSAAS prohormone has been reported in a variety of anatomical regions, including endocrine organs of the gut and brain and particularly the pituitary and hypothalamus (18, 35, 36). Although these initial reports do not distinguish between hypothalamic substructures, *in situ* hybridization for proSAAS in the mouse brain (www.brain-map.org) shows intense staining in cell bodies along the ventral medial portion of the SCN (37), a region consistent with RHT innervation of retinorecipient neurons (3).

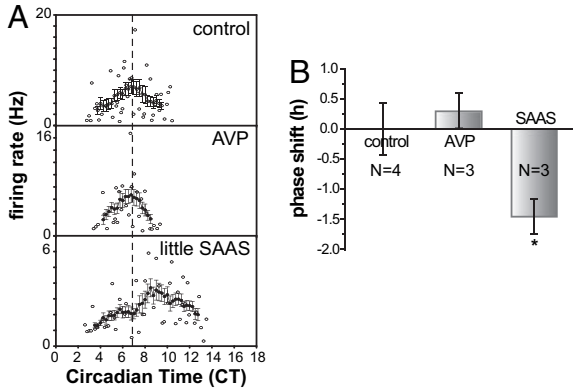

Fig. 5. Application of little SAAS induces a phase delay. (*A*) Exogenous microdrop application of little SAAS to the SCN coronal slice at CT 14 induces a phase delay of spontaneous peak firing rates of SCN neurons. Control single-unit activity graphs typically peak around CT 7 (*top*). Application of AVP as a negative control has no effect on peak firing time (*middle*), whereas little SAAS shifts phase by an average 1.5 h (*bottom*). Open circles, single units; filled circles, running mean activity. (*B*) Summary graph comparing phase shifts. Numbers are sample sizes. Error bars indicate standard deviation. $^{**}P < 0.01$ one-way ANOVA with Tukey post hoc test.

Combining the chemical profiles of peptides found within the brain with information on peptide secretion helps select the most promising unknown and known peptides for further studies. For example, unique peaks that exhibit an interesting stimulation-dependent release pattern are selected for further chemical characterization and biological assay, e.g., in this case, for circadian function. Obtaining such complementary information provides a directed screen for the structural elucidation and functional discovery of novel peptides and thus enables a new range of studies investigating the interplay of complex sets of signaling molecules in peptidergic neuronal networks that are becoming well defined.

Methods

Reagents. The MALDI matrixes α-cyano-4-hydroxycinnamic acid (CHCA) and 2, 5-dihydroxybenzoic acid were mixed in 70% acetonitrile (ACN) with 0.01% TFA. SPE bead elutions were performed with 70% ACN/H_2O. Little SAAS and AVP peptides for circadian phase assays were obtained from Phoenix Pharmaceuticals. Reagents were obtained from Sigma-Aldrich.

Animals. SCN-containing slices were prepared from 6- to 12-week-old inbred Long-Evans/BluGill rats (LE/BluGill, http://pga.mcw.edu/pga-bin/strain_desc.cgi). Rats were entrained to a daily 12-h:12-h light:dark cycle. CT in slices was projected from the light schedule to which the rats were entrained, in which the time of ''lights on'' was designated as CT 0. Subjective day corresponded to CT 0–12, and subjective night was defined as CT 12–24. Protocols for animal care and procedures were approved by the University of Illinois at Urbana–Champaign Laboratory Animal Care Advisory Committee and in full compliance with federal guidelines for the humane care and treatment of animals.

SCN Brain Slice Preparation. Animals were killed by guillotine during subjective daytime, and brain slices (500 μm) were prepared using a tissue chopper or a Vibratome (Leica Microsystems). Coronal brain slices and horizontal hypothalamic brain slices with attached optic nerves were prepared. Brain slices were maintained in a brain slice chamber perfused with EBSS and supplemented with 24.6 mM of glucose, 26.2 mM of NaHCO3, and 2.5 mg/l of gentamicin and were saturated with 95% O_2/5% CO_2 at 37°C, pH 7.4. Phenol red indicator interferes with neuropeptide collections and was excluded from EBSS.

Electrophysiology of the SCN Brain Slice. Single-unit spontaneous activity of SCN neurons was recorded, as described previously (38). Activity was measured in 4-min bins. Averages of firing rates and standard deviations were plotted versus time to determine the CT of peak activity for SCN neurons. Stimulation of the optic nerves was performed with wire electrodes connected to an S6 isolated pulse stimulator (Grass Technologies). Stimulation was performed at CT 14 for 5 min at 1V, 10 Hz with 0.2-ms pulse duration.

SCN Extraction and High-Performance Liquid Chromatographic Separation. SCN punches were prepared from coronal brain slice preparations, washed in EBSS, and immediately added to acidified acetone (40 μl) solutions for 40 min before freezing at −80 °C. Before high-performance liquid chromatography was performed, acetone was evaporated with a Thermo Savant SpeedVac concentrator (Thermo Electron Co.) for 10 min and replaced gradually with H_2O. Separations were performed with a Waters CapLC instrument (Waters Co.), and 5 ml of extraction supernatant was loaded onto a PLRP-S SPE microbore column (Supelco) and then eluted over the course of 40 min with a gradient of 0–80% solvent B (0.01% [vol/vol] TFA, 0.08% formic acid [vol/vol] in ACN) in solvent A (0.01% [vol/vol] TFA, 0.1% [vol/vol] formic acid in water). Fractions were spotted at 40-sec intervals onto a MALDI target plate for subsequent analyses.

SPE Bead Sampling of Secreted Peptides. Single resin ''D'' beads (Millipore Co.) were ''wetted'' in 50% ACN and equilibrated in EBSS. Activated beads were transferred between solutions or brain slice tissues by hand-held borosilicate capillary pipettes (World Precision Instruments) with pulled tips beveled to approximately 200 μm in diameter. Positioning on tissue surfaces was accomplished by hand with ×10–25 magnification.

Following sample collection, the beads were rinsed of salts, transferred to gold-coated MALDI target plates for sample elution (Applied Biosystems Inc.) and rinsed first with 70% ACN/H_2O (0.2 μl), followed by a second rinse of 70% ACN/H_2O containing saturated CHCA MALDI matrix (0.2 μl). Peptide signal was maximized by concentrating the peptide into a smaller area by coating the surface of the target with a stretched layer of Parafilm® M (Pechiney Plastic Packaging, Inc.) with holes of approximately 100 μm in each sample spot. As the eluant evaporated, the localized region of exposed metal concentrated analytes to an area similar to the irradiation area of the MALDI laser. The hydrophobic film was sealed to the target surface by convectional heating at 88°C for approximately 5 min. After the addition of MALDI matrix to the sample spot, MALDI TOF MS was performed (as described later) on prestimulation and stimulation samples. These mass spectra then were compared for stimulation-dependent peaks of interest.

SPE Pipette Sampling of Releasates. C_{18} Zip Tip® pipettes (Millipore) were ''wetted'' by aspiration with 50% ACN and equilibrated in EBSS immediately before use. Wetted pipettes were connected via Tygon tubing (Saint-Gobain Performance Plastics Co.) to a Harvard Apparatus (Harvard Biosience) syringe pump and a Hamilton gastight syringe (Hamilton Company). Pipettes were mounted to a micromanipulator for precise positioning of the SPE tips above the SCN region of the brain slice surface. The inner diameters of the pipette tips measured 500 μm and were sufficient to cover SCN tissue regions by area. Collections were performed by running the pump in negative mode, pulling extracellular samples across the SPE material at a rate of 0.2 μl/min. Secreted peptides were observed following stimulation with sample collections lasting 5 min, but typically the most complete and mass-resolved release profiles were obtained with 10- to 15-min collections; pipette collections lasted 15 min unless otherwise noted. After sample collection, pipettes were removed, cleared of EBSS, and aspirated with Millipore H_2O to rinse salts. Peptide samples were eluted successively with 4 μl of 70% and 100% ACN onto MALDI target plates (Applied Biosystems) modified as described previously, or prespotted PAC384 AnchorChips (Bruker Daltonics) for MS analyses.

MALDI TOF MS. MALDI TOF MS was performed with an Ultraflex II (Bruker Daltonics) mass spectrometer. Releasate mass spectra from SPE pipette samples were present in amounts sufficient for reflectron acquisition with MALDI TOF MS, producing isotopically resolved analyte mass peaks within 50 ppm of theoretical values (Table 1). Analyte-limited samples obtained from beads typically were measured in linear mode with parameters favoring sensitivity over mass accuracy in the spectral acquisition. Accordingly, many bead releasates were detected as average masses. Each spectrum is an average of 100–200 laser pulses. Mass spectra were calibrated with external peptide standards. For related samples, such as those from 24-h collection experiments, the samples were plated consecutively on the same MALDI target and were analyzed consecutively on the same day without altering instrument settings to promote uniformity for relative comparisons of the same analyte peak at different time intervals. The signal-to-noise ratio for each analyte is plotted to reduce random differences in intensities between samples; plots of peak area and peak heights show little difference. Peptide peaks were required to be at least 3σ to background noise for inclusion in Table 1.

Peptide Sequence Confirmation: MS/MS Analyses. The analyses were performed using more than one MS/MS approach. For most samples, MS/MS was accomplished with an Ultraflex II MALDI TOF/TOF mass spectrometer in ''LIFT'' mode. Both liquid chromatographic fractions and releasate samples were applied to a prespotted target plate and CHCA MALDI matrix applied. Parent ions were analyzed first for accurate mass with internal standards before fragmenting into product ion spectra. MS/MS spectra were analyzed using the accompanying Flex Analysis and Biotools software packages (Bruker Daltonics). Confirmation of sequence identity required the matching of at least three successive fragment ions in MS/MS mode.

Additionally, endogenous peptide mixtures were separated and analyzed by capillary liquid chromatography MS/MS. The separation was performed on a PicoFrit ProteoPep II C18 column (New Objective) driven by NanoLC-1D pumps (Eksigent) at 300 nL/min. Eluting peptides were sprayed into a high-resolution 7-Tesla linear ion trap quadrupole Fourier transform mass spectrometer (Thermo Scientific) over the course of a 90-min gradient. Peptides were fragmented in a data-dependent manner, and the resulting precursor and fragment ion masses were searched against an in-house database of rat neuropeptides using ProSightPC software (Thermo Scientific). All peptides retrieved from this custom database matched to within 5 ppm of their predicted intact masses, and all fragment ions matched to within 10 ppm of their predicted fragment ion masses.

ACKNOWLEDGMENTS. We thank Dr. Jennifer Mitchell for help with the physiological testing of AVP. This report is based on work supported by National Institute on Drug Abuse Awards P30 DA 018310 to the UIUC Neuroproteomics Center on Cell to Cell Signaling and R01 DA 017940 (to J.V.S.), and National Heart, Lung, and Blood Institute Award R01 HL086870 (to M.U.G.).

1. Moore RY, Eichler VB (1972) Loss of a circadian adrenal corticosterone rhythm following suprachiasmatic lesions in the rat. *Brain Res* 42:201–206.
2. Stephan FK, Zucker I (1972) Circadian rhythms in drinking behavior and locomotor activity of rats are eliminated by hypothalamic lesions. *Proc Natl Acad Sci USA* 69:1583–1586.
3. Abrahamson EE, Moore RY (2001) Suprachiasmatic nucleus in the mouse: Retinal innervation, intrinsic organization and efferent projections. *Brain Res* 916:172–191.
4. Ralph MR, Foster RG, Davis FC, Menaker M (1990) Transplanted suprachiasmatic nucleus determines circadian period. *Science* 247:975–978.
5. Hatcher NG, Richmond TA, Rubakhin SS, Sweedler JV (2005) Monitoring activity-dependent peptide release from the CNS using single-bead solid-phase extraction and MALDI TOF MS detection. *Anal Chem* 77:1580–1587.
6. Hatcher NG, Sweedler JV (2008) *Aplysia* bag cells function as a distributed neurosecretory network. *J Neurophysiol* 99:333–343.
7. Jakubowski JA, Hatcher NG, Xie F, Sweedler JV (2006) The first gamma-carboxyglutamate-containing neuropeptide. *Neurochem Int* 49:223–229.
8. Jing J, *et al.* (2007) From hunger to satiety: Reconfiguration of a feeding network by *Aplysia* neuropeptide Y. *J Neurosci* 27:3490–3502.
9. Moore RY, Speh JC, Card JP (1995) The retinohypothalamic tract originates from a distinct subset of retinal ganglion cells. *J Comp Neurol* 352:351–366.
10. Shibata S, Moore RY (1993) Neuropeptide Y and optic chiasm stimulation affect suprachiasmatic nucleus circadian function in vitro. *Brain Res* 615:95–100.
11. Earnest DJ, Sladek CD (1986) Circadian rhythms of vasopressin release from individual rat suprachiasmatic explants in vitro. *Brain Res* 382:129–133.
12. Gillette MU, Reppert SM (1987) The hypothalamic suprachiasmatic nuclei: Circadian patterns of vasopressin secretion and neuronal activity in vitro. *Brain Res Bull* 19:135–139.
13. Akabayashi A, *et al.* (1994) Diurnal rhythm of galanin-like immunoreactivity in the paraventricular and suprachiasmatic nuclei and other hypothalamic areas. *Peptides* 15:1437–1444.
14. Davies JS, Carter DA, Wells T (2004) Photic stimulation inhibits growth hormone secretion in rats: A hypothalamic mechanism for transient entrainment. *Endocrinology* 145:2950–2958.
15. Kim DY, *et al.* (2001) Substance P plays a critical role in photic resetting of the circadian pacemaker in the rat hypothalamus. *J Neurosci* 21:4026–4031.
16. Meyer-Spasche A, Reed HE, Piggins HD (2002) Neurotensin phase-shifts the firing rate rhythm of neurons in the rat suprachiasmatic nuclei in vitro. *Eur J Neurosci* 16:339–344.
17. van den Pol AN, Tsujimoto KL (1985) Neurotransmitters of the hypothalamic suprachiasmatic nucleus: Immunocytochemical analysis of 25 neuronal antigens. *Neuroscience* 15:1049–1086.
18. Fricker LD, *et al.* (2000) Identification and characterization of proSAAS, a granin-like neuroendocrine peptide precursor that inhibits prohormone processing. *J Neurosci* 20:639–648.
19. Che FY, Biswas R, Fricker LD (2005) Relative quantitation of peptides in wild-type and Cpe(fat/fat) mouse pituitary using stable isotopic tags and mass spectrometry. *J Mass Spectrom* 40:227–237.
20. Dowell JA, Heyden WV, Li L (2006) Rat neuropeptidomics by LC-MS/MS and MALDI-FTMS: Enhanced dissection and extraction techniques coupled with 2D RP-RP HPLC. *J Proteome Res* 5:3368–3375.
21. Svensson M, Skold K, Svenningsson P, Andren PE (2003) Peptidomics-based discovery of novel neuropeptides. *J Proteome Res* 2:213–219.
22. Romijn HJ, Sluiter AA, Pool CW, Wortel J, Buijs RM (1997) Evidence from confocal fluorescence microscopy for a dense, reciprocal innervation between AVP-, somatostatin-, VIP/PHI-, GRP-, and VIP/PHI/GRP-immunoreactive neurons in the rat suprachiasmatic nucleus. *Eur J Neurosci* 9:2613–2623.
23. van Leeuwen FW, Swaab DF, de Raay C (1978) Immunoelectronmicroscopic localization of vasopressin in the rat suprachiasmatic nucleus. *Cell Tissue Res* 193:1–10.
24. Prosser RA, Gillette MU (1989) The mammalian circadian clock in the suprachiasmatic nuclei is reset in vitro by cAMP. *J Neurosci* 9:1073–1081.
25. Shibata S, Tsuneyoshi A, Hamada T, Tominaga K, Watanabe S (1992) Effect of substance P on circadian rhythms of firing activity and the 2-deoxyglucose uptake in the rat suprachiasmatic nucleus in vitro. *Brain Res* 597:257–263.
26. Gillette MU, Mitchell JW (2002) Signaling in the suprachiasmatic nucleus: Selectively responsive and integrative. *Cell Tissue Res* 309:99–107.
27. Hannibal J, *et al.* (1997) Pituitary adenylate cyclase-activating peptide (PACAP) in the retinohypothalamic tract: A potential daytime regulator of the biological clock. *J Neurosci* 17:2637–2644.
28. Piggins HD, Marchant EG, Goguen D, Rusak B (2001) Phase-shifting effects of pituitary adenylate cyclase activating polypeptide on hamster wheel-running rhythms. *Neurosci Lett* 305:25–28.
29. Aton SJ, Colwell CS, Harmar AJ, Waschek J, Herzog ED (2005) Vasoactive intestinal polypeptide mediates circadian rhythmicity and synchrony in mammalian clock neurons. *Nat Neurosci* 8:476–483.
30. Shinohara K, Honma S, Katsuno Y, Abe H, Honma K (1994) Circadian rhythms in the release of vasoactive intestinal polypeptide and arginine-vasopressin in organotypic slice culture of rat suprachiasmatic nucleus. *Neurosci Lett* 170:183–186.
31. Gamble KL, Allen GC, Zhou T, McMahon DG (2007) Gastrin-releasing peptide mediates light-like resetting of the suprachiasmatic nucleus circadian pacemaker through cAMP response element-binding protein and Per1 activation. *J Neurosci* 27:12078–12087.
32. Karatsoreos IN, Yan L, LeSauter J, Silver R (2004) Phenotype matters: Identification of light-responsive cells in the mouse suprachiasmatic nucleus. *J Neurosci* 24:68–75.
33. Fortenberry Y, Hwang JR, Apletalina EV, Lindberg I (2002) Functional characterization of proSAAS: Similarities and differences with 7B2. *J Biol Chem* 277:5175–5186.
34. Mzhavia N, *et al.* (2002) Processing of proSAAS in neuroendocrine cell lines. *Biochem J* 361:67–76.
35. Feng Y, Reznik SE, Fricker LD (2001) Distribution of proSAAS-derived peptides in rat neuroendocrine tissues. *Neuroscience* 105:469–478.
36. Sayah M, Fortenberry Y, Cameron A, Lindberg I (2001) Tissue distribution and processing of proSAAS by proprotein convertases. *J Neurochem* 76:1833–1841.
37. Lein ES, *et al.* (2007) Genome-wide atlas of gene expression in the adult mouse brain. *Nature* 445:168–176.
38. Ding JM, *et al.* (1994) Resetting the biological clock: Mediation of nocturnal circadian shifts by glutamate and NO. *Science* 266:1713–1717. span style='font-size:10.0pt'